Carboranyl Units Bringing Unusual Thermal and Structural Properties to Hybrid Materials Prepared by Sol−Gel Process

Arántzazu González-Campo,[†,§] Bruno Boury,[‡] Francesc Teixidor,[†] and Rosario Núñez*[,†]

Institut de Ciència de Materials de Barcelona CSIC, Campus UAB, E-08193 Bellaterra, Spain, and Laboratoire Chimie Moleculaire et Organisation du Solide, UMR 5637, Université de Montpellier II, Place E. Bataillon, F-34095 Montpellier Cedex 5, France

Received March 17, 2006. Revised Manuscript Received June 29, 2006

Strategies for the preparation of carboranyl-containing hybrid materials by hydrolytic sol−gel process were investigated with carboranyl-containing poly-trialkoxysilyl precursors: 1,2-$[(CH_2)_3Si(OEt)_3]_2$-1,2-$C_2B_{10}H_{10}$ (**P1**) and 1-R-2-$Si[(CH_2)_2Si(OEt)_3]_3$-1,2-$C_2B_{10}H_{10}$ (R = Me, **P2** or Ph, **P3**). When **P1** is used, the integrity of the precursor is preserved whatever is the catalyst (F^-, H^+), while for **P2** and **P3**, cleavage of the $C_{cluster}$−Si bond is observed with F^- and OH^- as catalysts. Such Si−$C_{cluster}$ bond cleavage leads to porous hybrid materials templated by the carborane, which is further eliminated from the material and totally recovered. In contrast, nonporous materials are obtained when carborane is preserved in the materials. Part of this hybrid material exhibits a lamellar structure in relation to the presence of the carborane units. In dry air, high thermal stability is observed for such materials and results in a very limited oxidation of the material at 1200 °C (weight gain of <5%). In an inert atmosphere, high thermal stability combined with several chemical transformations leads to a limited weight loss, graphitization, and oxide and under-oxide mixtures. Materials were characterized by IR, solid-state NMR (^{29}Si,^{13}C), porosimetry, X-ray diffraction, SEM, TEM, TGA, and XPS.

Introduction

Boron cluster ligands provide structural and bonding possibilities distinct from conventional organic ligands.[1] The exceptional characteristics exhibited by these icosahedral carboranes,[2,3] such as electron-withdrawing properties,[4] low nucleophilicity, chemical inertness, thermal stability, highly polarizable *σ*-aromatic character, and high hydrophobicity have stimulated research on the development of novel polymeric materials incorporating these boron clusters.[5] Thermal treatment of *o*-carborane at 465−500 °C[6] and in a flow system at 600 °C[7] produces the meta isomer in high yield, while higher temperatures give an equilibrium mixture of *p*-carborane and its meta isomer. High-temperature stable hybrid polymers containing carborane clusters bonded to siloxane groups have been reported.[3b,8] These have been used as oxidative protection coatings or ceramic polymeric materials that exhibit outstanding thermal and thermo-oxidative properties compared to other silicon polymers.[9] Despite their potential application related to these properties, a limited number of carborane-containing hybrid materials are known, and their behavior in the preparation of sol−gel hybrid materials remains to be tested. As for other class II hybrid materials where the "organic" moiety is covalently linked to the Si−O−Si network,[10] the organization, level of condensation, porosity, and composition are the key parameters to keep the carboranyl unit accessible to reactivity. Therefore, we have been attracted to developing class II organic−inorganic hybrid materials incorporating *o*-carborane moieties, and we recently reported the preparation and characterization of hybrid materials obtained from a trichlo-

* To whom correspondence should be addressed. E-mail: rosario@icmab.es.
† Institut de Ciència de Materials de Barcelona CSIC.
‡ Université de Montpellier II.
§ Enrolled in the UAB PhD program.

(1) (a) Grimes, R. N. In *Comprehensive Organometallic Chemistry II, Vol. 1*; Abel, E. W., Stone, F. G. A., Wilkinson, G., Eds.; Pergamon: Oxford, 1995; pp 373−430. (b) Grimes, R. N. *Coord. Chem. Rev.* **2000**, *200/202*, 773. (c) Saxena, A. K.; Hosmane, N. S. *Chem. Rev.* **1993**, *93*, 1081. (d) Saxena, A. K.; Maguire, J. A.; Hosmane, N. S. *Chem. Rev.* **1997**, *97*, 2421.
(2) (a) Grimes, R. N. *Carboranes*; Academic Press: New York, 1970; p 54. (b) Hawthorne, M. F. *Current Topics in the Chemistry of Boron*; Kabalka, G. W., Ed.; The Royal Society of Chemistry: Cambridge, U.K., 1994; p 207. (c) Hawthorne, M. F. *Advances in Boron Chemistry*; The Royal Society of Chemistry: Cornwall, U.K., 1997; p 261. (d) King, R. B. *Chem. Rev.* **2001**, *101*, 1119.
(3) (a) Bregadze, V. I. *Chem. Rev.* **199**2, *92*, 209. (b) Plesek, J. *Chem. Rev.* **1992**, *92*, 269.
(4) (a) Teixidor, F.; Núñez, R.; Viñas, C.; Sillanpää, R.; Kivekäs R. *Angew. Chem.* **2000**, *112* (23), 4460−4462. *Angew. Chem., Int. Ed.* **2000**, *39* (23), 4290−4292. (b) Núñez, R.; Teixidor, F.; Viñas, C.; Farrás, P.; Kivekäs, R.; Sillanpää. R. *Angew. Chem.* **2006**, *118*, 1292−1294. *Angew. Chem., Int. Ed.* **2006**, *45*, 1270−1272.
(5) Lu, S.-Y.; Hamerton, I. *Prog. Polym. Sci.* **2002**, *27*, 1661, and references therein.
(6) Grafstein, D.; Dvorak, J. *Inorg. Chem.* **1963**, *2*, 1128.
(7) Papetti, S.; Obeland, C.; Heying, T. L. *Ind. Eng. Chem. Prod. Res. Dev.* **1966**, *5*, 334.
(8) (a) Papetti, S.; Schaeffer, B. B.; Gray, A. P.; Heying, T. L. *J. Polym. Sci., Part A: Polym. Chem.* **1966**, *4*, 1623. (b) Henderson, L. J.; Keller, T. M. *Macromolecules* **1994**, *27*, 1660. (c) Sundar, R. A.; Keller, T. M. *J. Polym. Sci., Part A: Polym. Chem.* **1997**, *35*, 2387. (d) Houser, E. J.; Keller, T. M. *J. Polym. Sci., Part A: Polym. Chem.* **1998**, *36*, 1969. (e) Dougherty, T. K.: U.S. Patent 235,264,285, 1993. (f) Houser E. J.; Keller, T. M. *Macromolecules* **1998**, *31*, 4038. (g) Dvornic, P. R.; Lenz, R. W. In *High Temperature Siloxane Elastomers*; Huethig & Wepf Verlag: New York, 1990. (h) Beckham, H. W.; Keller, T. M. *J. Mater. Chem.* **2002**, *12*, 3363.
(9) (a) Keller, T. M. *Carbon* **2002**, *40*, 2002. (b) Ichitani, M.; Yonezawa, K.; Okada, K.; Sugimoto, T. *Polym. J.* **1999**, *31*, 908. (c) Kimura, H.; Okita, K.; Ichitani, M.; Sugimoto, T.; Kuroki, S.; Ando, I. *Chem. Mater.* **2003**, *15*, 355. (d) Kolel-Veetil, M. K.; Beckham, H. W.; Keller, T. M. *Chem. Mater.* **2004**, *16*, 3162. (e) Kolel-Veetil, M. K.; Keller, T. M. *J. Polym. Sci., Part A: Polym. Chem.* **2006**, *44*, 147.

10.1021/cm060648w CCC: $33.50
Published on Web 08/15/2006

Scheme 1. Synthesis of Precursors: (A) P1, (B) P2, and P3

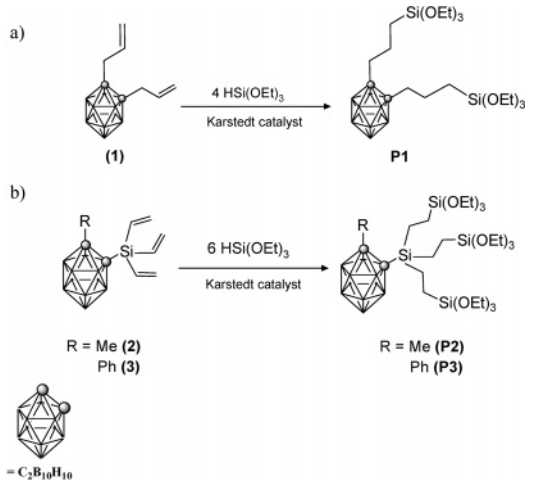

rosilyl precursor.[11] In this report we focus on the elaboration of carborane-containing hybrid materials from sol−gel hydrolysis/polycondensation of carborane-containing organosilanes that are suitable for the immobilization of the carborane in an inorganic matrix with high chemical and thermal stability. Therefore, we envisage the preparation of new carboranyl-bridged polysilsesquioxanes from different precursors by hydrolysis/condensation of $-Si(OEt)_3$ groups included in the precursor structure. In this report we investigate the strategies and limitation for the introduction of the carborane units in such class II hybrid materials. We also check the structural organization of the material since the neutral carboranyl unit has weaker self-organization properties[12] than those reported recently (polar units, ionic units, and H-bonding units) and that exhibits self-organized structure.[10h] Finally, because of the thermal stability of the clusters, we investigate the chemical and structural evolutions of such carboranyl-containing material upon thermal treatment in inert and dry air atmosphere.

Results and Discussion

Synthesis and Characterization of Precursors. Precursor **P1** was obtained from the hydrosilylation reaction of the allyl groups in 1,2-$(CH_2CH{=}CH_2)_2$-1,2-$C_2B_{10}H_{10}$,[11] using an excess of $HSi(OEt)_3$ in the presence of Karstedt catalyst at room temperature for 2 h (Scheme 1a). Precursors **P2** and **P3** were prepared in a manner similar to the corresponding vinyl-containing-carborane groups 1-(CH_3)-2-$Si(CH{=}CH_2)_3$-1,2-$C_2B_{10}H_{10}$ and 1-(C_6H_5)-2-$Si(CH{=}CH_2)_3$-1,2-$C_2B_{10}H_{10}$[13] (Scheme 1b). According to the ^1H and ^{13}C NMR analysis, the hydrosilylation mostly occurs in the β-position and leads to the precursors in very high yield (≈99%). The ^1H NMR spectra show two peaks at 3.84 and 1.25 ppm due to the −OEt functions; the corresponding peaks in the ^{13}C NMR spectra are displayed at 58.9 and 18.6 ppm. The ^{29}Si NMR spectrum of **P1** shows one peak at −46.7 ppm, whereas two resonances are exhibited for **P2** and **P3** corresponding to $Si-C_{cluster}$ (10.6 ppm for **P2** and 11.6 ppm for **P3**) and C−SiOEt (−46.6 ppm for **P2** and −46.4 ppm for **P3**). Some differences are observed in the $^{11}B\{^1H\}$ NMR spectra patterns of the precursors: 2:8 for **P1**, 1:1:6:2 for **P2**, and 1:1:4:2:2 for **P3**.

Scheme 2. Preparation of Xerogels X1A (TBAF) and X1B (HCl)

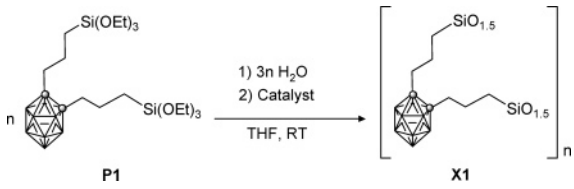

Scheme 3. Preparation of Xerogels X2 [A(TBAF), B(NaOH), C(HCl)] and X3 [A(TBAF), B(NaOH), C(HCl)]

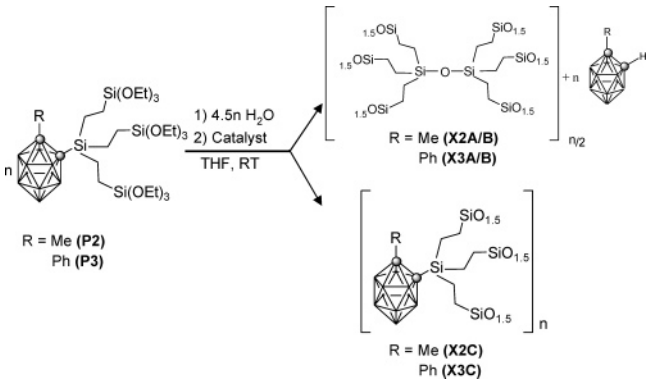

Table 1. Experimental Conditions Xerogels Obtained in THF

xerogel	precursor	precursor (mol L^{-1})	catalyst	catalyst (mol L^{-1})	gelation time (h)
X1A	**P1**	1	TBAF	0.02	192
X1B	**P1**	1	HCl	0.6	4320
X2A	**P2**	1	TBAF	0.03	0.33
X2B	**P2**	1	NaOH	0.03	1824
X2C	**P2**	1	HCl	0.45	744
X3A	**P3**	1	TBAF	0.03	0.41
X3B	**P3**	1	NaOH	0.03	648
X3C	**P3**	1	HCl	0.44	1296

Preparation of Xerogels by Sol−Gel Process. The hydrolysis-polycondensation of all precursors was carried out at room temperature (20−25 °C), in THF solutions (1 M) in the presence of a catalyst with the stoichiometric amount of deionized water at pH = 6−7. Three standard catalysts were tested to activate the hydrolysis/polycondensation reaction: a nucleophile (TBAF), an acid (HCl), and a base (NaOH). The ideal equations and the conditions corresponding to the polycondensation of the precursors are represented in Schemes 2 and 3 and in Table 1. Under these conditions, no precipitation was observed, and after formation of the gels, they were allowed to age for 7 days, washed, and dried. The

(10) (a) Loy, D. A.; Shea, K. J. *Chem. Rev.* **1995**, *95*, 1431. (b) Avnir, D. *Acc. Chem. Res.* **1995**, *28*, 328. (c) Corriu, R. J. P.; Leclercq, D. *Angew. Chem., Int. Ed. Engl.* **1996**, *35*, 4001. (d) Shea, K. J.; Loy, D. A. *Chem. Mater.* **2001**, *13*, 3306. (e) Cerveau, G.; Corriu, R. J. P.; Framery, E. *Chem. Mater.* **2001**, *13*, 3373. (f) Lu, Z.-L.; Lindner, E.; Hermann, A. *Chem. Rev.* **2002**, *102*, 3543. (g) Boury, B.; Corriu, R. *Chem. Commun.* **2002**, 795. (h) Shea, K. J.; Moreau, J.; Loy, D. A.; Corriu, R. J. P.; Boury, B. *Functional Hybrid Materials*; Sánchez, C., Gómez-Romero, P., Eds.; Wiley-VCH: Weinheim, 2004; p 50.
(11) González-Campo, A.; Núñez, R.; Viñas, C.; Boury, B. *New J. Chem.* **2006**, *30*, 546.
(12) (a) Fox, M. A.; Hughes, A. K. *Coord. Chem. Rev.* **2004**, *248*, 457. (b) Planas, J. G.; Viñas, C.; Teixidor, F.; Comas-Vives, A.; Ujaque, G.; Lledós, A.; Light, M. E.; Hursthouse, M. B. *J. Am. Chem. Soc.* **2005**, *127*, 15976.
(13) González-Campo, A.; Núñez, R.; Viñas, F.; Teixidor, R.; Kivekäs, R. Sillanpää, R. Unpublished work.

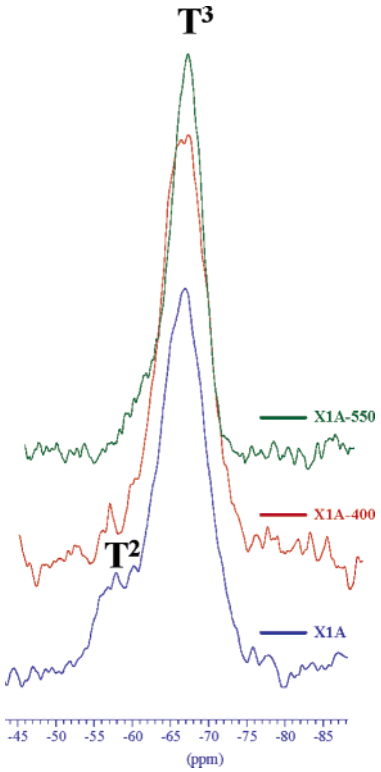

Figure 1. ^{29}Si CP MAS NMR spectra for **X1A**, **X1A-400**, and **X1A-550**.

resulting insoluble and brittle materials were grounded to powders. The gelation time depends clearly on the type of precursor and the catalyst used. In general, the formation of gels was faster for higher concentration of hydrolyzable Si−OEt function in the precursor (**P2**, **P3**) and when TBAF was used as catalyst.

Spectroscopic, Structural, and Textural Characterization of Xerogels Obtained from P1. The persistence of the cluster, the presence of the organic spacer, and the condensation of the Si−OEt functions are confirmed by the spectroscopic data: the IR spectra of **X1A** and **X1B** exhibit strong bands at 2590 cm^{-1} (B−H stretching), at 2966−2876 and 1250 cm^{-1} (ν_{-CH2-}), at 1093 cm^{-1} (Si−O−Si stretching), and very low intensity bands at 3400 and 3600 cm^{-1} (ν_{SiO-H}). The ^{13}C CP MAS NMR spectra of xerogels reveal three resonances around 37, 24, and 12 ppm (−CH_2−CH_2−CH_2− Si alkyl spacer), a broad peak centered at 80.4 ppm due to $C_{cluster}$ atoms (C_c), and two peaks of low intensity, at 59.0 and 18.3 ppm, due to residual Si(OEt) groups. The ^{29}Si CP MAS NMR spectra for both xerogels display two resonances, at −57 and −66 ppm, attributed to T^2 and T^3 substructures, respectively (Figure 1).[11] The level of condensation (LC) was estimated by deconvolution of spectra and using the formula LC = $^1/_3T^1 + {}^2/_3T^2 + 1T^3$ (Table 2).[14] An exceptionally high LC (≈94%) is measured for materials prepared with **P1** using HCl or TBAF as catalyst, the level of T^3 being considerably higher than the one of T^2 subunits. No Q^n units were detected and we concluded that both ^{29}Si and ^{13}C CP MAS NMR data support that Si−C bonds were not cleaved during the condensation process. Organization of the solids at the micro- and mesoscopic scale was checked by X-ray powder diffraction analysis, which present two broad signals corresponding to a *d* spacing of 6.4 and 15.7 Å for **X1A** and 6.4 and 14.5 Å for **X1B** (Figure 2). These signals are clearly related to the presence of the organo-carboranyl unit and in a first attempt of interpretation, signals at 15.7 and 14.5 Å might be considered as the 001 order and those at 6.4 Å as 002 order of a lamellar structure. Compared to other hybrid materials with short-range order organization, in these xerogels the signal at 3.8 Å, generally attributed to the Si−O−Si contribution, is not clearly observed.[15] These XRD patterns are very similar to those previously reported for hybrid materials prepared from 1,2-[$(CH_2)_3SiCl_3$]$_2$-1,2-$C_2B_{10}H_{10}$ that exhibited a lamellar structure.[11] Thus, a lamellar structure with a short-range order organization due to a periodic structure with alternating organo-carboranyl units and silica layers may be proposed.[11] By nitrogen adsorption/desorption isotherms,[16] a low specific surface area (0−11 m^2 g^{-1}) was obtained in both cases. This is consistent with a lamellar highly packed structure and with previous observations related to the presence of long alkyl groups in this type of material.[10a,11] SEM images of **X1A** exhibit dense and heterogeneous particles (Figure 3a). Transmission electronic microscopy (TEM) studies reveal great heterogeneity in terms of microscopic structure for xerogel **X1A**, which presents a large amorphous part, and a minor part with high

Table 2. ^{29}Si CP MAS NMR Data of Xerogels

	^{29}Si NMR CP-MAS								
	T^0		T^1		T^2		T^3		
xerogel	ppm	%	ppm	%	ppm	%	ppm	%	L.C.[a] (%)
X1A		0		0	−57.7	17	−66.9	83	94
X1B		0		0	−57.6	22	−66.2	78	93
X2A		0		0	−57.3	47	−64.4	53	
X2B	−46.1	12	−53.3	35	−57.5	30	−64.7	23	
X2C		0	−51.5	6	−57.1	30	−64.3	64	86
X3A	−47.0	2	−50.7	3	−57.1	88	−65.0	7	
X3B		0	−49.9	24	−57.0	45	−64.9	31	
X3C		0		0	−57.0	53	−64.1	47	82

[a] Level of condensation calculated according to the general equation L.C. = [0.5(T^1 area) + 1.0(T^2 area) + 1.5(T^3 area)]/1.5.

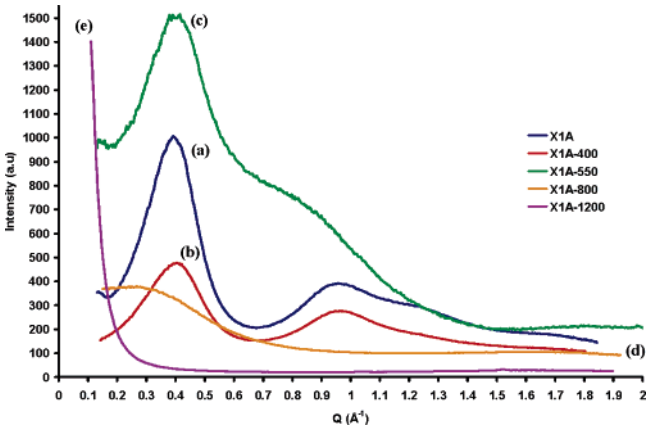

Figure 2. XRD diagram for xerogel **X1A** before and after the thermal treatment at different temperatures under argon: (a) **X1A**, (b) **X1A-400**, (c) **X1A-550**, (d) **X1A-800**, and (e) **X1A-1200**.

(14) Cervau, G.; Corriu, R.; Lepeytre J. P. C.; Mutin, H. P. *J. Mater. Chem.* **1998**, *8*, 2707.

(15) Boury, B.; Corriu, R. J. P. *Chem. Rec.* **2003**, *3*, 120.

(16) (a) Lowell, S.; Shields, J. E. In *Powder Surface and Porosity*; Chapman and Hall: London, 1984. (b) Gregg, S. J.; Sing, K. S. W. In *Adsorption, Surface Area and Porosity*; Academic Press: London, 1982.

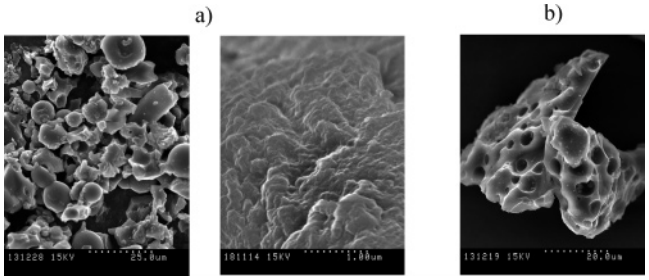

Figure 3. SEM images of **X1A** at different temperatures: (a) **X1A** and (b) **X1A-550**.

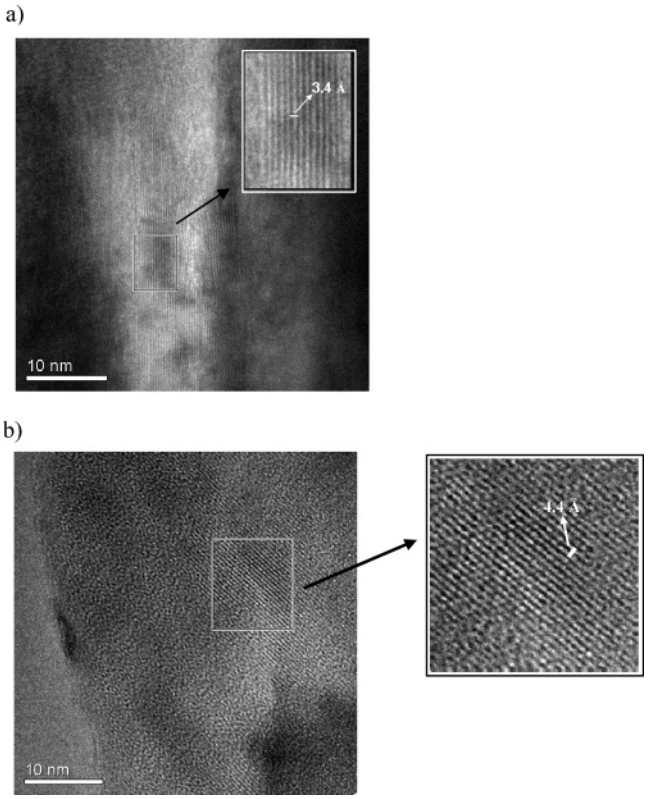

Figure 4. TEM images of (a) **X1A** and (b) **X1A-550.**

Table 3. Binding Energies (eV) in the Core-Level X-ray Photoelectron Spectra of C 1s, B 1s, Si 2p, and O 1s for X1A, X1A-550, X1A-1200 under Ar, and X1A-1200 under Air

solid	C 1s	B 1s	Si 2p	O 1s
X1A	284.9	189.4	102.5	532.3
X1A-550	284.7, 286.3, 288.0	190.8	103.4	531.5
X1A-1200 (Ar)	285.0, 287.2, 289.3	194.4	105.1	534.3
X1A-1200 (O_2)	282.7, 284.7, 286.3, 287.6, 289.0	194.2	104.5, 102.4, 99.6	533.7

level of organization. TEM images presented in Figure 4a confirm the layered structure for the organized part of the material. An interlayer spacing of 3.4 Å can be estimated and might agree with the (004) order with respect to the high-intensity peak (001) observed in the XRD pattern. Additionally, the X-ray photoelectron spectroscopy (XPS) gives some information about the bonding within the different elements on the material surface (Table 3). The binding energy of C 1s core levels found in **X1A** are approximately 284.9 eV assigned to C−C aliphatic functions. The binding energy for B 1s is 189.4 eV assigned to B−H bonds; for Si 2p it is 102.5 eV, assigned to Si−O; and for O 1s it is 532.3 eV. The peak at 189.4 eV corresponding to B−H bonds confirms the presence of the carborane cluster in the material.

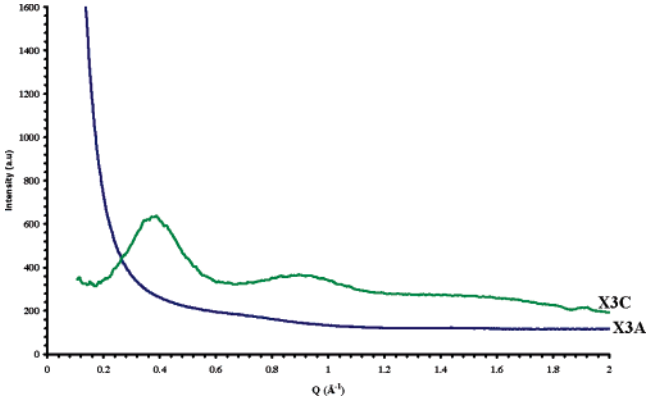

Figure 5. XRD diagrams for xerogels **X3A** and **X3C**.

Spectroscopic, Structural, and Textural Characterization of Xerogels Obtained from P2 and P3. Three different catalysts were tested, TBAF for **X2A** and **X3A,** NaOH for **X2B** and **X3B**, and HCl for **X2C** and **X3C** (Table 1). Clear differences must be made between **X2C** and **X3C** on one hand and **X2A**, **X2B**, **X3A**, and **X3B** on the other hand, since for the latter ones there is evidence that $Si-C_c$ bonds cleavage occurs during sol−gel processes. First, for **X2A**, **X2B**, **X3A**, and **X3B**, methyl-*o*-carborane and phenyl-*o*-carborane were recovered at 90%, with respect to the respective starting precursors (**P2** and **P3**), from the organic solvents used for washing the gels. IR spectra of those gels do not exhibit bands around 2590 cm^{-1} (B−H stretching); however, they show a strong band around 1037 and 1076 cm^{-1} (Si−O−Si stretching). The ^{13}C CPMAS NMR spectra of these xerogels show peaks of low intensity, at 59.0 and 18.3 ppm (residual nonhydrolyzed Si−OEt groups), a broad resonance at 6.4 ppm (CH_2 groups of the vinyl chain), and no signal at 80.4 ppm ($C_{cluster}$ atoms). Finally, ^{29}Si CP MAS NMR spectra of **X2A** and **X2B** show signals corresponding to T^n units, *n* depending on the precursor and condition: for **X2A** (T^2 and T^3), for **X2B** and **X3A** (T^0, T^1, T^2, and T^3), and for **X3B** (T^1, T^2, and T^3 subunits) (values in Table 2). However, the presence of other signals is consistent with the cleavage of the $C_{cluster}-Si$ bond during the sol−gel process, which involves a nucleophilic attack by fluoride ions or strong bases, such as NaOH, on the very electrophilic silicon atom.[17] Low-intensity signals in the region of −100 to −110 ppm are consistent with Q^n substructures resulting from Si−C hydrolysis. In addition, a signal at 13.2 ppm was attributed to the Si atom of the moiety $O[\boldsymbol{Si}[(CH_2)_2SiO_{0.5}]_3]_2$ resulting from hydrolysis and condensation of C_c-Si to give −Si−O−Si− functions (Scheme 3). Because of the $Si-C_c$ cleavage, the level of condensation (LC) of these xerogels has not been considered here. The X-ray diffraction patterns of xerogels **X2A**, **X2B**, **X3A** (Figure 5), and **X3B** do not exhibit any Bragg's peaks, indicating the formation of a completely amorphous material. By gas sorption porosimetry, those xerogels have high specific surface area. Xerogel **X2A** shows a specific surface area of approximately 570 $m^2\ g^{-1}$

(17) (a) Gomez, F. A.; Hawthorne, M. F. *J. Org. Chem.* **1992**, *57*, 1384. (b) Xie, Z.; Wang, S.; Yang, Q.; Mak, T. C. W. *Organometallics* **1999**, *18*, 1578. (c) Xie, Z.; Wang, S.; Yang, Q.; Mak, T. C. W. *Organometallics* **1999**, *18*, 2420. (d) Xie, Z. *Acc. Chem. Res.* **2003**, *36*, 1.

with a porosity of H3 type according to the De Boer classification,[18] with an average pore diameter of 32 Å. This solid presents largely mesoporous contribution (79%) without narrow pore size distribution and weak microporous contribution (21%). Similarly, **X3A** presents a specific surface area of 170 $m^2\ g^{-1}$ with a porous size of 28 Å, being mainly mesoporous. All these data indicate that the formation of porous hybrid organic−inorganic materials from **P2** and **P3** was clearly related to the efficiency of the catalyst action for removing the carborane clusters. In this case, the porosity could be accomplished using the templating effect of the methyl- or phenyl-*o*-carboranes that are later removed.[19] This preliminary result could provide an alternative way for preparing porous hybrid materials by the controlled elimination of carborane from the material, exploiting the sensibility of C_c−Si bonds. However, a fine-tuning of the porosity will require, first, control of the formation of the Si−O−Si network followed, second, by the Si−C_c cleavage.

Xerogels **X2C** and **X3C** prepared in acidic conditions are completely different and they exhibit strong bands at 2590 cm^{-1} due to the B−H stretching by IR analysis. The ^{13}C CP MAS NMR spectra of **X2C** shows one resonance around 25.0 ppm (C_c−CH_3) and **X3C** exhibits broad resonances around 130 ppm (C_6H_5 group). Additional peaks corresponding to Si−CH_2 are observed around 6.0 ppm. The ^{29}Si CPMAS NMR spectra of **X2C** (mostly of T^2 subunits) and **X3C** (T^2 and T^3 substructures in a similar ratio) indicate high levels of condensation of 86% and 83%, respectively (Table 2). All these data agree with the preservation of the Si−$C_{cluster}$ covalent bond during the sol−gel process. Moreover, the XRD diagram of **X3C** shows two broad signals corresponding to a *d* spacing of 16.5 and 6.98 Å (Figure 5), which are very close to those observed for xerogel **X1A**. This result clearly confirms that a lamellar structure with a short-range order organization could be assumed for **X3C** and is an obvious verification that signals observed are related to the presence of the carboranyl units. Xerogels **X2C** and **X3C** were nonporous materials with specific surface areas of <10 m^2g^{-1} by nitrogen adsorption/desorption isotherms.

Thermal Treatment of Carboranyl-Containing Hybrid Material X1. The carboranyl-bridged hybrid materials **X1A** and **X1B** exhibit good thermal stability up to 450 °C under argon, as other similar hybrid materials with phenyls or arylenes-bridged polysilsesquioxanes.[20] Xerogels lose weight by two waves (2.1% + 4.1%) in the range 100−450 °C, which is usually attributed to desorption of residues and the final condensation of the material. Between 450 and 800 °C an important weight loss of ≈16.5% occurs. Heating up to 1200 °C leaves a ceramic char with a 77% yield (Figure 6).

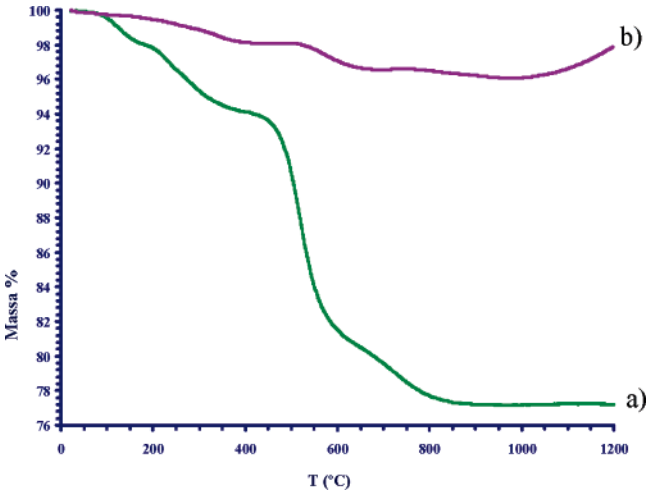

Figure 6. TGA analyses for xerogel **X1A**: (a) under argon and (b) under dry air.

Table 4. BET and XRD of Carboranyl-Containing Hybrids: X1A before and after Thermal Treatment, X1B, X2C, and X3C

material	BET ($m^2\ g^{-1}$)	XRD (Å)
X1A	<10	15.7/6.4
X1B	11	14.5/6.4
X1A-400	<10	15.0/6.4
X1A-550	265	16.2
X1A-800	22	22.4
X1A-1200	<10	
X2C	<10	16.4/6.7
X3C	<10	16.5/6.9

Considering that the elimination of all organic spacers would lead to a theoretical 35% weight loss, the conservation of an elevated organics quantity in the material is obvious and this behavior, different from other hybrid materials of this type, suggests that the carborane provides a high stabilizing effect to the material during the thermolysis in an inert atmosphere.

To obtain more detailed information of this thermal behavior, characterizations of **X1A** were done after annealing at 400, 550, 800, and 1200 °C, under an argon flow, followed by washing with THF and drying, to remove all the soluble residual compounds before characterization:

(a) Up to 400 °C, the recovered material **X1A-400** does not show significant changes in the X-ray diagram and in the specific surface area with respect to the started xerogel **X1A** (Table 4, Figure 2). However, a higher level of condensation according to the ^{29}Si CP MAS spectra is observed, showing only a broad peak at −66.0 ppm corresponding to T^3 subunits and suggesting a LC ≈ 100% (Figure 1). The ^{13}C CP MAS NMR spectrum confirms the presence of the alkyl spacers and C_c atoms. At this temperature, the residual condensation has occurred without apparent alteration of the initial structure.

(b) **X1A-400** was heated to 550 °C and **X1A-550** was recovered after a weight loss of ≈8%, which could be attributed to the elimination of a part of the organic units. The IR spectrum shows a large band at 2586 cm^{-1} due to ν(BH) of the *closo* cluster, and bands of lower intensity in the region 2950−2880, which corroborate the presence of alkyl groups. The ^{29}Si CP MAS NMR spectrum is similar to that of **X1A-400,** exhibiting only a broad band at −66.0 ppm (T^3) (Figure 1). Therefore, the Si atoms are still bonded

(18) Sing, K. S. W.; Everett, D. H.; Haul, R. A. W.; Moscou, L.; Pierotti, R. A.; Rouquerol, J.; Siemieniewska, T. *Pure Appl. Chem.* **1985**, *57*, 603.
(19) (a) Boury, B.; Chevalier, P.; Corriu, R. J. P.; Delord, P.; Moreau, J. J. E.; Wong-Chiman, M. *Chem. Mater.* **1999**, *11*, 281. (b) Boury, B.; Corriu, R. J. P.; Le Strat, V. *Chem. Mater.* **1999**, *11*, 2796. (c) Boury, B.; Corriu, R. J. P. *Adv. Mater.* **2000**, *12*, 989.
(20) (a) Shea, K. J.; Loy, D. A.; Webster, O. *J. Am. Chem. Soc.* **1992**, *114*, 6700. (b) Loy, D. A.; Jamison, G. M.; Baugher, B. M.; Myers, S. A.; Assink, R. A.; Shea, K. J. *Chem. Mater.* **1996**, *8*, 656. (c) Cerveau, G.; Corriu, R. J. P.; Fischmeister-Lepeytre, C. *J. Mater. Chem.* **1999**, *9*, 1149.

to the C atoms from alkyl groups at this temperature. However, the ^{13}C CP MAS NMR spectrum exhibits new resonances compared to that of **X1A-400**: a new peak at 128.9 ppm was attributed to the presence of unsaturated C═C in the material and that at −3.9 ppm assigned to a CH_3 group bonded to a Si atom. Our hypothesis is that thermal treatment leads to the formation of partially $-CH_2{=}CH_2$ and $CH_3SiO_{1.5}$ units by rearrangement of the $CH_2CH_2CH_2SiO_{1.5}$ radicals that result from one $C_{cluster}-C$ bond cleavage. The XRD diagram of **X1A-550** exhibits substantial differences with respect to the starting **X1A**; only one broad band corresponding to *d* spacing 16.2 Å was observed, while the band corresponding to *d* spacing of 6.2 Å is hardly noticeable (Table 4, Figure 2). Additionally, a shoulder of low intensity with a *d* spacing of 7.9 Å is observed. Simultaneously, **X1A-550** exhibits a high specific surface area of 265 $m^2\ g^{-1}$, being mainly microporous. The SEM images of **X1A-550** reveal the general aspect of the material, which suggests that plastic deformations occur at the same time with gas elimination (Figure 3b). Finally, the TEM analyses confirm the microporosity with an approximated pore size of 4.4 Å (Figure 4b). To investigate the bonding in **X1A-550** and compare it with that in the starting **X1A** xerogel, the XPS bonding spectra were measured (Table 3). The C 1s spectrum shows a main peak at 284.7 assigned to C−C aliphatic bonds, and other peaks at 286.3 and 288.0 eV are attributed to C−O and C═O bonds, respectively. The B 1s core level spectrum shows a peak at 190.8 eV, shifted about 1.4 eV toward a higher binding energy with respect to the **X1A**. This result could be indicative that some changes have occurred in the carborane cluster with the temperature; anyway the interpretation is that no B−O bonds are presented in this material. The Si 2p spectrum shows a peak at 103.4 eV typical of silicon atoms bonding to three oxygen atoms.[21]

This thermal behavior is unusual for related organic−inorganic hybrid materials; thus, it might be attributed to the presence of the carborane cluster. All these results indicate that the *closo* cluster is still present in the material, but were not conclusive whether the *o*-carborane has isomerized to *m*-carborane. At this point two experiments were carried out in order to prove the possible isomerization process. Xerogel **X1A** was placed in a sealed tube and heated at 550 and 650 °C in the oven under vacuum. The recovered materials were washed with THF and the soluble residues monitored by ^1H and ^{11}B NMR. The residue after heating at 550 °C does not show signals related to the cluster. However, at 650 °C, the ^{11}B NMR spectrum exhibits a set of broad resonances at −1.9, −5.3, −8.8, −10.3, −11.9, −13.4, and −15.6 ppm, which cannot be attributed either to *o*- or *m*-carborane. Thus, at this temperature, a percentage of the carborane is not covalently bonded to the siloxane matrix due to the complete $C_{cluster}-CH_2$ bonds cleavage, and this free carborane proves that the cluster rearrangement process is undergoing.

(c) Xerogel **X1A-800** is obtained after heating **X1A-550** up to 800 °C, with an additional weight loss of ≈6%. The XRD diagram shows only a very broad band with *d* spacing of 22.4 Å, and the second band corresponding to a *d* spacing of 3.7 Å (Si−O−Si) is practically missing (Figure 2). The ATR spectrum does not present the band corresponding to the B−H stretching, indicating that the *closo* cluster has been completely degraded at this temperature. In addition, broad bands at 1300 and 1035 cm^{-1} attributed to B−O and Si−O, respectively, are observed. The **X1A-800** is a nonporous material exhibiting a low specific surface area of ca. 22 m^2/g. Evolution of X-ray diffraction and specific surface area may be tentatively interpreted by taking into account the fact that first the carborane subunit can react at this temperature with the matrix made of Si−O−Si and Si−C oxycarbide network and second that this oxycarbide may be above its glass transition at this temperature. With respect to that, the carborane units no longer exist in the medium as such, and the porosity observed at 550 °C collapses due to the softening of the matrix.

(d) **X1A-800** was heated to 1200 °C to give **X1A-1200** as an amorphous and nonporous black residue, with a specific surface area $<10\ m^2\ g^{-1}$. The XRD diagram does not show any Bragg's peaks for both large and small angles (Figure 2). The elemental analysis using X-ray photoelectron spectroscopy (XPS) determined an atomic concentration of O (43.02%), C (35.08%), Si (11.37%), and B (10.53%) in the material surface. The curve fittings (Figure 7) give some information about the bonding within the different elements; the binding energy of C 1s core levels found in **X1A-1200** are 285.0, 287.2, and 289.3 eV assigned to C−C aliphatics, C−O, and C═O functions, respectively. These have also been observed in carbon−fiber polymer composites or graphitic structures.[22] The binding energy for the O 1s is 534.3 eV, for B 1s 194.4 eV assigned to B−O bonds, and for Si 2p 105.1 eV assigned to Si−O in silica.[23] The absence of binding energy at 187 eV corresponding to B−H bonds in the XPS analysis revealed the complete oxidation of the carborane group and the presence of different oxides (B_2O_3 and SiO_2) in the ceramic.[9b] Microscopic analyses reveal a heterogeneous medium at different scales: scanning electron microscopy (SEM) analysis of **X1A-1200** shows the presence of droplets of insoluble mineral material $<1\ \mu m$ in diameter that seem to have been exuded at the surface of the bulk (Figure 8). Interestingly, the TEM images of these micrometer-size droplets reveals highly dense and amorphous materials possibly rich in boron (Figure 9a). At a lower scale, nanoparticles of 2−10 nm appear embedded in the amorphous matrix possibly made of boron crystallized as shown by transmission electron microscopy (Figure 9b). In other parts of the material, the presence of graphite structures are clearly observed in Figure 9c, where the distance between the layer planes approaches 3.3 Å.[24] These results agree well with the previously described surface XPS analyses for the **X1-1200**.

(21) Morra, M.; Occiello, E.; Marola, R.; Garbasi, F.; Humphrey, P.; Johnson, D. *J. Colloid Interface Sci.* **1990**, *137*, 11.

(22) (a) Sie, Y.; Sherwood, M. A. *Chem. Mater.* **1989**, *1*, 427. (a) Darmstadt, H.; Roy, C.; Kaliaguine, S. *Carbon* **1994**, *32*, 1399. (c) Lee, J. G.; Haddon, R. C.; Reucroft P. J. *Appl. Surf. Sci.* **2001**, *18*1, 121. (d) Hou, P. X.; Bai, S.; Yang, Q. H.; Liu, C.; Cheng, H. M. *Carbon* **2002**, *40*, 81.

(23) Campos- Martín, J. M. In *Técnicas de Análisis y Caracterización de Materiales*; Faraldos, M., Goberna, C., Eds.; Consejo Superior de Investigaciones Científicas: Madrid, Spain, 2002; p 491.

(24) Renlund, G. M.; Prochazka, S. *J. Mater. Res.* **1991**, *6*, 2723.

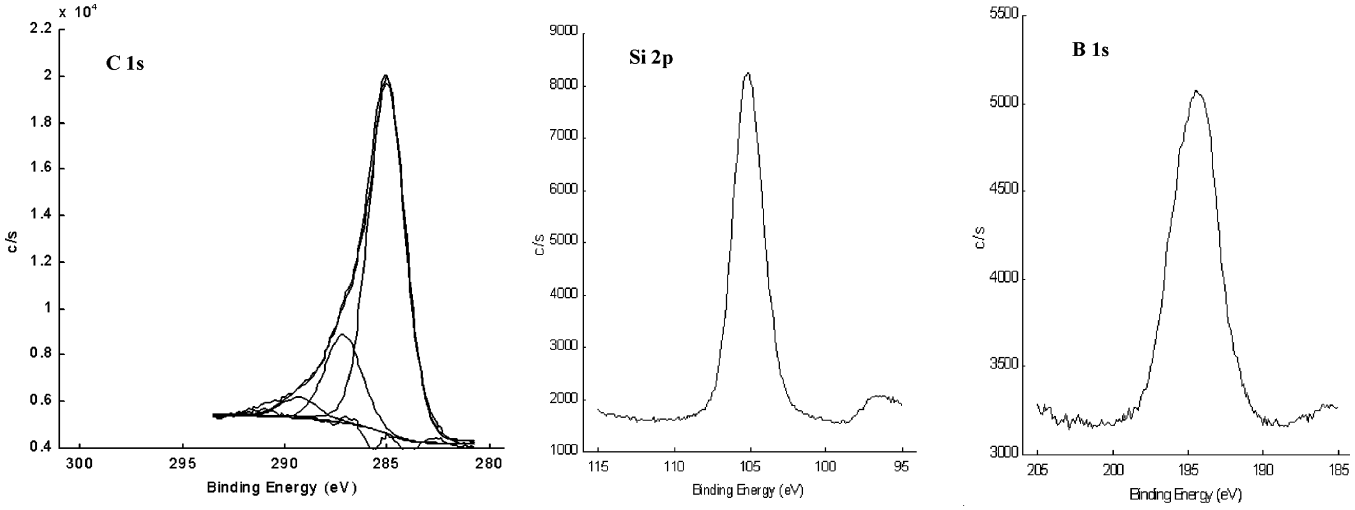

Figure 7. C 1s, B 1s, and Si 2p binding energy envelopes in the X-ray photoelectron spectra of **X1A-1200** under argon.

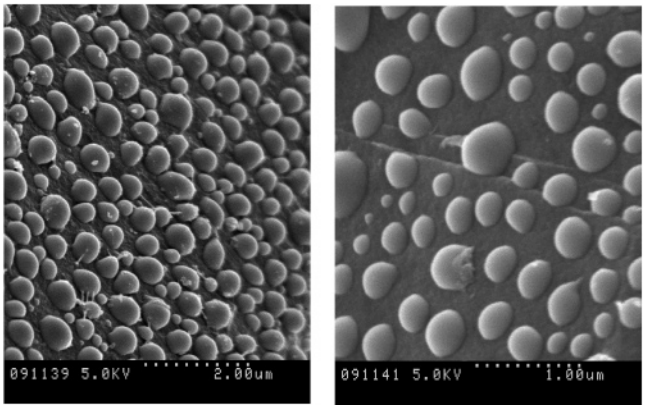

Figure 8. Scanning electron microscopy (SEM) images of **X1A-1200** under argon.

Finally, under dry air, the TGA analysis of **X1A** shows a completely different behavior: after an usual weight loss of 1.9% between 20 and 350 °C, a weight loss of 2% occurs in two waves up to 1000 °C and then a weight increase of 2% occurs from 1000 °C up to 1200 °C to yield a black char (Figure 6). DTA curve indicates that exothermic processes are occurring, probably due to oxidation reactions. All together, the weight loss of **X1A** in air up to 1200 °C is lower than 2%. This very low weight loss is surprising if considering the following oxidation phenomena that can occur: carborane $\Rightarrow B_2O_3$ (+72.7%), $CSiO_{1.5} \Rightarrow SiO_2$ (+4.8%) and $(-CH_2- + C) \Rightarrow CO_2 + H_2O$ (−35.7%).[9a,25] Indeed, the formation of a SiO_2/B_2O_3 glass by complete oxidation of the initial material would imply a weight increase of 41.8%. Therefore, it can be concluded that only a very small proportion of the material is oxidized in this process. Here again a high stability of the material at high temperature under dry air seems related to the presence of the carboranyl subunit. However, it must be mentioned that this oxidation effect is highly dependent on the particles size and surface expose to oxidizing agent; in the present case

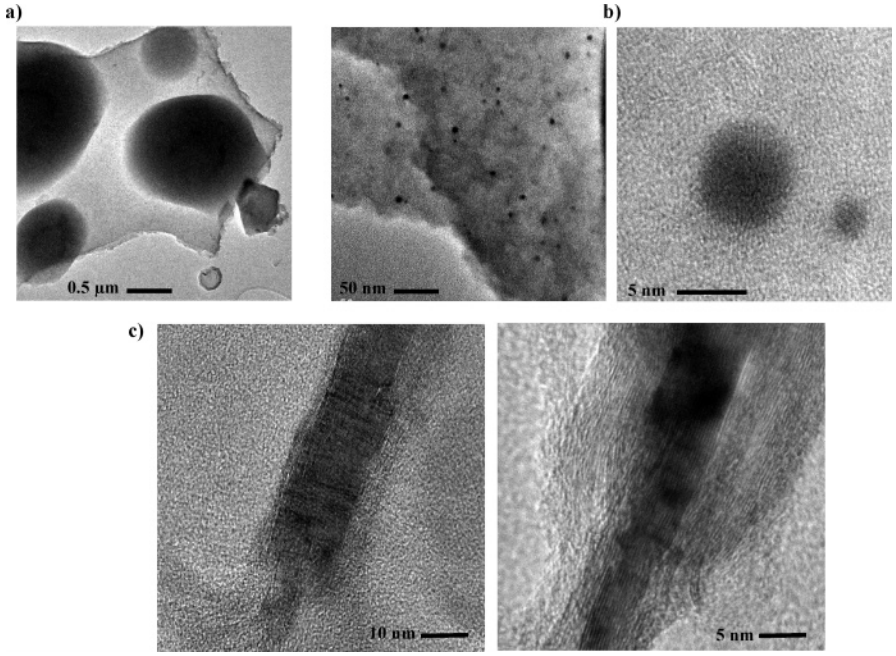

Figure 9. TEM images of **X1A-1200** under argon: (a) image showing micrometer droplets, (b) image showing nanoparticles of 2−10 nm, and (c) graphitic structures observed in the material.

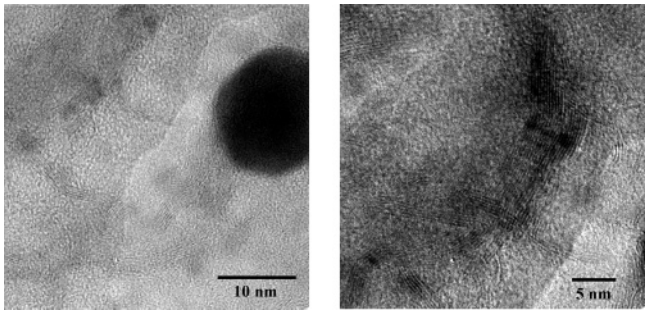

Figure 10. TEM images for char obtained after heating **X1A** up to 1200 °C under dry air.

the high stability is certainly also related to the very low surface area of the material. The ATR spectrum of the char obtained at 1200 °C exhibits very intense bands at 1400 and 1035 cm^{-1} attributed to B−O and Si−O, respectively. Additionally, X-ray photoelectron spectroscopy (XPS) bonding spectra show some differences with respect to the **X1A-1200** obtained under argon (see Table 3, Figure 11). The C 1s spectrum shows a very broad band that, after deconvolution, presents five peaks. The main peaks are located approximately at 284.7 and 287.6 eV, which can be associated with C−C and C−O bonds, respectively, and corroborate the presence of graphitic structures. The peak at 282.7 eV could be assigned to C−Si bonds, typical of silicon carbides (Figure 11). Besides, the Si 2p spectrum shows a main peak near 104.5 eV that can be assigned to Si−O, which is overlapping another less intense peak at 99.6 eV probably due to Si−C bonds typical of silicon carbide (Figure 11).[26] The binding energy for the B 1s is 194.2 eV assigned to B−O bonds in B_2O_3 and for the O 1s is 533.7 eV which can be associated with oxygen in Si−O bonds. Finally, the TEM analysis reveals that the structure rearranges into discrete layer planes indicative of graphite structures (Figure 10),[24] and the results agree well with the surface XPS analyses of the solid. Likewise, the presence of such graphite structure is rather surprising since the sample is kept under air at 1200 °C.

Conclusions

Organo-carboranyl polysilsesquioxanes have been demonstrated to be a versatile class of materials. They can be prepared from precursors that integrate carboranyl subunits and $Si(OEt)_3$ groups that can be polymerized by the sol−gel process. Due to the high sensitivity of the C_c−Si bond, the sol−gel process must be achieved in non-nucleophilic conditions or through the use of an organic spacer between C_c and Si atoms, to avoid C_c−Si cleavage and keep the carborane as an integrated unit of the hybrid material. In this respect, all carboranyl-containing xerogels were nonporous solids with a high level of condensation and with mostly a short-range order organization, detected in the form of lamellar structure, and attributed to the presence of the rigid carborane in the material. Furthermore, adaptation of the experimental conditions should emphasize the formation of the detected lamellar structure homogeneously in the material. Contrarily, organic−inorganic hybrids obtained after removal of the carborane cluster are completely amorphous and mesoporous materials, with high specific surface areas. In this case, the porosity could be accomplished using the templating effect of the carborane, after its controlled elimination from the material. Another alternative way for preparing porous hybrid materials exploiting the sensibility of the C_c−Si bond to the nucleophilic attack is under study. Thermal evolution of carborane-containing hybrid materials in an inert atmosphere reveals the following: (a) inertness up to 450 °C, (b) formation of micropores between 450 and 550 °C, with limited weight loss and

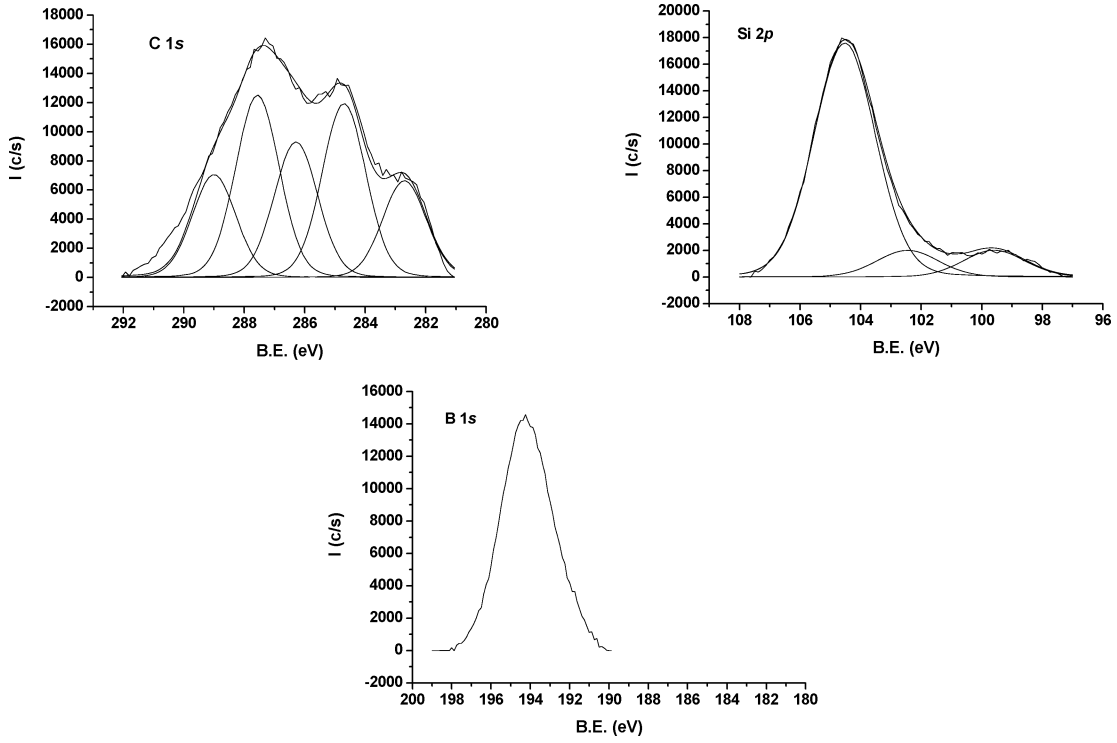

Figure 11. Binding energy envelopes in the X-ray photoelectron spectra of **X1A-1200** under dry air.

feasible carborane cluster modification (rearrangement or starting isomerization), and (c) up to 1200 °C closing of the porosity without weight loss, formation of graphite structures, and dense nanoparticles. Thermal evolution of the same material in an oxidative atmosphere leads to a very small weight increase (<5%) due to a very limited oxidation process that leaves a boron-rich material with the presence of graphite structures.

Experimental Section

Materials. All reactions were carried out under an atmosphere of purified argon using standard Schlenk techniques. Solvents were purified, dried, and distilled by standard procedures. $HSi(OEt)_3$ and Karstedt platinum catalyst (3−3.5% Pt) were purchased from ABCR. TBAF, NaOH, and HCl were used as received from Aldrich. 1,2-$(CH_2CH{=}CH_2)_2$-1,2-$C_2B_{10}H_{10}$, 1-CH_3-2-$Si(CH{=}CH_2)_3$-1,2-$C_2B_{10}H_{10}$ and 1-C_6H_5-2-$Si(CH{=}CH_2)_3$-1,2-$C_2B_{10}H_{10}$ were prepared according to literature procedures.[11,13]

Instrumentation. Infrared spectra were measured in NaCl or KBr pellets on a ThermoNicollet AVATAR 320 FT-IR. Attenuated Total Reflection (ATR) was measured on a Bruker Tensor 27 using an accessory Specac NKII Golden Gate. ^{1}H NMR, ^{1}H{^{11}B} NMR (300.13 MHz), ^{11}B NMR (96.29 MHz), ^{13}C{^{1}H} NMR (75.47 MHz), and ^{29}Si{^{1}H} NMR (59.62 MHz) spectra were recorded on a Bruker ARX 300 spectrometer. NMR spectra were measured in $CDCl_3$ solution at room temperature. Chemical shifts for ^{11}B NMR were referenced to external $BF_3{\cdot}OEt_2$ and those for ^{1}H NMR, ^{13}C NMR, and ^{29}Si NMR were referenced to Me_4Si. ^{29}Si CP MAS NMR (at 79.49 MHz) and ^{13}C CP MAS NMR (at 100.63 MHz) spectra were obtained on a Brucker Advance ASX400 using a CP MAS sequence. Thermogravimetric analysis (TGA) of the network materials was performed on a Netzsch STA 409 PC/PG under a 50 mL min^{-1} argon flow. Samples were heated from 20 to 1200 °C at 5 °C/min. X-ray powder diffraction measurements were performed using a spectrometer with a rotating copper anode with an OSMIC monochromator system and an "Image Plate 2D" detector working with the Cu Kα (λ = 1.542 Å) radiation and a beam size of 0.5 × 0.5 mm and acquisition time of 40−50 min. Samples were previously crushed and placed in a Lindeman tube (1 mm diameter). The specific surface areas, porosity, volume, and the pore size distribution were determined by analyzing the N_2 adsorption/desorption isotherms according to the BET method using a Micromériticcs Gémini III 2375 et ASAP 2010. Scanning electron microscopy (SEM) images were performed in an HITACHI S-570 microscope. Transmission electron microscopy (TEM) images were produced with a JEOL JEM 2011 (200 kV) microscope. Elemental analyses were performed in the analytical laboratory using a Flash EA 1112 Series microanalyzer. X-ray photoelectron spectra are obtained on a PHYSICAL ELECTRONICS mod. 5701 (ESCA) Imaging XPS System.

Synthesis of 1,2-$[(CH_2)_3Si(OCH_2CH_3)_3]_2$-1,2-$C_2B_{10}H_{10}$ (P1). In a Schlenk flask under argon, 1,2-$(CH_2CH{=}CH_2)_2$-1,2-$C_2B_{10}H_{10}$ (1.326 g, 5.9 mmol), $HSi(OCH_2CH_3)_3$ (4.5 mL, 23.6 mmol), and Karstedt's catalyst (10 μL, 0.021 mmol) were mixed and stirred for 2 h at room temperature. Evaporation of the volatiles and the excess of $HSi(OCH_2CH_3)_3$ at 50 °C gave 3.23 g of a yellow oil. Yield: ≈99%. ^{1}H{^{11}B} NMR (δ (ppm)): 3.84 (q, O−C**H**$_2$, ^3J(H,H) = 6.9 Hz, 12H), 2.20 (t, C_c−C**H**$_2$, ^3J(H,H) = 7.7 Hz, 4H), 1.66 (m, CH_2−C**H**$_2$−CH_2, 4H), 1.25 (t, CH_2−C**H**$_3$, ^3J(H,H) = 6.9 Hz, 18H), 0.62 (t, C**H**$_2$−Si, ^3J(H,H) = 6.9 Hz, 4H). ^{11}B NMR (δ (ppm)): −4.9 (d, ^1J(B,H) = 145 Hz, 2B), −10.7 (8B). ^{13}C{^{1}H} NMR (δ (ppm)): 80.1 (**C**$_c$), 58.9 (O−**C**H$_2$), 38.0 (C_c−**C**H$_2$), 23.7 (CH_2−**C**H$_2$−CH_2), 18.6 (CH_2−**C**H$_3$), 10.7 (C**H**$_2$−Si). ^{29}Si{^{1}H} NMR (δ (ppm)): −46.7.

Synthesis of 1-(CH_3)-2-$Si[(CH_2)_2Si(OCH_2CH_3)_3]_3$-1,2-$C_2B_{10}H_{10}$ (P2). In a Schlenk flask under argon, 1-(CH_3)-2-$Si(CH{=}CH_2)_3$-1,2-$C_2B_{10}H_{10}$ (0.620 g, 2.3 mmol), $HSi(OCH_2CH_3)_3$ (2.7 mL, 14.2 mmol), and Karstedt's catalyst (8 μL, 0.017 mmol) were mixed and heated to reflux. Then, the mixture was stirred for 91 h at room temperature. Evaporation of the volatiles and the excess of $HSi(OCH_2CH_3)_3$ at 50 °C gave 1.75 g of a yellow oil. Yield: ≈99%. ^{1}H{^{11}B} NMR (δ (ppm)): 3.84 (q, O−C**H**$_2$, ^3J(H,H) = 7.0 Hz, 18H), 2.04 (s, C_c−C**H**$_3$), 1.25 (t, CH_2−C**H**$_3$, ^3J(H,H) = 7.0 Hz, 27H), 0.91 (m, Si−C**H**$_2$−, 6H) 0.60 (m, Si−C**H**$_2$, 6H). ^{11}B NMR (δ (ppm)): 1.5 (d, ^1J(B,H) = 130 Hz, 1B), −3.9 (d, ^1J(B,H) = 160 Hz, 1B), −7.3 (d, ^1J(B,H) = 153 Hz, 6B), −9.6 (2B). ^{13}C-{^{1}H} (δ (ppm)): 76.2 (**C**$_c$), 71.9 (**C**$_c$), 58.9 (O−**C**H$_2$), 26.4 (C_c−**C**H$_3$), 18.6 (CH_2−**C**H$_3$), 4.7 (Si−**C**H$_2$), 3.3 (Si−**C**H$_2$). ^{29}Si{^{1}H} NMR (δ (ppm)): 10.6 (C_c−**Si**), −46.6 (**Si**−O).

Synthesis of 1-(C_6H_5)-2-$Si[(CH_2)_2Si(OCH_2CH_3)_3]_3$-1,2-$C_2B_{10}H_{10}$ (P3). In a Schlenk flask under argon, 1-(C_6H_5)-2-$Si(CH{=}CH_2)_3$-1,2-$C_2B_{10}H_{10}$ (902 mg, 2.7 mmol), $HSi(OCH_2CH_3)_3$ (3.1 mL, 16.3 mmol), and Karstedt's catalyst (8 μL, 0.017 mmol) were mixed and stirred for 117 h at room temperature. Evaporation of the volatiles and the excess of $HSi(OCH_2CH_3)_3$ at 50 °C gave 2.23 g of a yellow oil. Yield: ≈99%. ^{1}H{^{11}B} NMR (δ (ppm)): 7.67−7.27 (m, C_6**H**$_5$, 5H), 3.84 (q, O−C**H**$_2$, ^3J(H,H) = 7.0 Hz, 18H), 1.25 (t, CH_2−C**H**$_3$, ^3J(H,H) = 7.0 Hz, 27H), 0.48 (m, Si−C**H**$_2$−C**H**$_2$−Si, 12H). ^{11}B NMR (δ (ppm)): 1.5 (d, ^1J(B,H) = 142 Hz, 1B), −3.7 (d, ^1J(B,H) = 145 Hz, 1B), −8.0 (d, ^1J(B,H) = 156 Hz, 4B), −10.1 (2B), −11.4 (d, ^1J(B,H) = 151 Hz, 2B). ^{13}C{^{1}H} (δ (ppm)): 131.3, 131.7, 130.8, 128.9 (**C**$_6$H$_5$), 83.5 (**C**$_c$), 76.5 (**C**$_c$), 58.9 (O−**C**H$_2$), 18.6 (CH_2−**C**H$_3$), 4.0 (Si−**C**H$_2$), 3.1 (Si−**C**H$_2$). ^{29}Si{^{1}H} NMR (δ (ppm)): 11.6 (C_c−**Si**), −46.4 (**Si**−O).

Preparation of Xerogels X1A and X1B. The preparation of xerogels was carried out according to the following general procedure; the **X1A** is given as an example. In a tube, 704 mg (1.27 mmol) of **P1** was dissolved in 637 μL of dried THF. Then, 637 μL of a solution containing 25 μL (25.5 μmol) of TBAF (1 M in THF), 69 μL (3.82 mmol) of H_2O, and 543 μL of dried THF were added. The mixture was then stirred for 10 s. After 192 h a gel was formed and kept 7 days for aging. The gel obtained was powdered and washed three times with ethanol, acetone, and diethyl ether and dried in a vacuum for 3 h to yield 372 mg of a white powder. Yield: 88%. FTIR (KBr, cm^{-1}): ν $(C-H)_{alkyl}$ 2966−2928, ν (B−H) 2590, δ $(C-H)_{alkyl}$ 1460, ν (Si−O−Si) 1093. ^{29}Si CP MAS NMR (δ (ppm)): −57.7 (T^2); −66.9 (T^3). ^{13}C CP MAS NMR (δ (ppm)): 80.4 (**C**$_c$), 59.0 (Si−O**C**H$_2$), 37.3 (**C**H$_2$), 23.7 (**C**H$_2$), 18.3 (OCH_2**C**H$_3$), 12.4 (**C**H$_2$). S_{Bet} < 10 m^2 g^{-1}. X-ray powder diffraction shows two very intense broad bands with *d* spacings of 15.7 and 6.4 Å.

X1B. Nine hundred milligrams (1.63 mmol) of **P1** in 1.63 mL of THF containing 41 μL (0.49 mmol) of HCl (37%) and 88 μL (4.89 mmol) of H_2O gave 452 mg of a gel after 4320 h. Yield: 84%. FTIR (KBr, cm^{-1}): ν $(C-H)_{alkyl}$ 2947−2876, ν (B−H) 2593, δ $(C-H)_{alkyl}$ 1460, ν (Si−O−Si) 1093. ^{29}Si CP MAS NMR (δ (ppm)): −57.6 (T^2); −66.2 (T^3). ^{13}C CP MAS NMR (δ (ppm)): 80.4 (**C**$_c$), 59.0 (Si−O**C**H$_2$), 37.3 (**C**H$_2$), 23.7 (**C**H$_2$), 18.3 (OCH_2**C**H$_3$), 12.4 (**C**H$_2$). S_{Bet} =11 m^2 g^{-1}. X-ray power diffraction shows two broad bands with *d* spacings of 14.5 and 6.4 Å.

X1A-400. The xerogel **X1A** was heated at 400 °C under an argon flow of 5 °C min^{-1}. The white solid produced was analyzed, indicating the complete condensation of the starting material **X1A**.

(25) Pehrsson, P.; Henderson, L. J.; Keller, T. M. *Surf. Interface. Anal.* **1996**, *24*, 145.
(26) Aoyama, T.; Sugii, T.; Ito, T. *Appl. Surf. Sci.* **1989**, *41*, 584.

FTIR (KBr, cm^{-1}): ν $(C-H)_{alkyl}$ 2939−2914, ν (B−H) 2586, δ $(C-H)_{alkyl}$ 1460, ν (Si−O−Si) 1031, 690. ^{29}Si CP MAS NMR (δ (ppm)): −66.0 (T^3). ^{13}C CP MAS NMR (δ (ppm)): 80.4 ($\mathbf{C}_c$), 37.3 ($\mathbf{C}H_2$), 23.7 ($\mathbf{C}H_2$), 13.1 ($\mathbf{C}H_2$). S_{Bet} = 3 m^2 g^{-1}. X-ray powder diffraction shows two broad bands with *d* spacings of 15.0 and 6.4 Å.

X1A-550. Xerogel **X1A-400** was heated to 550 °C under an argon atmosphere. The recovered white solid was analyzed. FTIR (KBr, cm^{-1}): ν $(C-H)_{alkyl}$ 2950−2880, ν (B−H) 2586, δ $(C-H)_{alkyl}$ 1460, ν (Si−O−Si) 1138, 774. ^{29}Si CP MAS NMR (δ (ppm)): −64.7 (T^3). ^{13}C CP MAS NMR (δ (ppm)): 128.9 (**C**═C), 71.0 ($\mathbf{C}_c$), 20.7 ($\mathbf{C}H_2$), −3.9 (OSi−$\mathbf{C}H_3$). S_{Bet} = 265 m^2 g^{-1}. X-ray powder diffraction shows one broad band with *d* spacing of 16.2 Å and two very low intensity bands corresponding to *d* spacings 7.9 and 3.9 Å.

X1A-800. Xerogel **X1A-550** was heated to 800 °C under an argon atmosphere. The recovered black solid was analyzed. ATR (cm^{-1}): ν $(C-H)_{alkyl}$ 2950−2880, ν (B−O) 1300, ν (Si−O−Si) 1035. ^{29}Si CP MAS NMR (δ (ppm)): −66.0 (T^3), 110 (Q^n). S_{Bet} = 22 m^2g^{-1}. X-ray powder diffraction shows one broad band with *d* spacing of 22.4 Å and a very low intensity band corresponding to *d* spacing 3.7 Å.

X1A-1200. Xerogel **X1A-800** was heated to 1200 °C under an argon atmosphere, a black residue being obtained. ATR (cm^{-1}): ν (B−O) 1376, ν (Si−O−Si) 1189, 1086. S_{Bet} < 10 m^2 g^{-1}. ^{11}B CPMAS NMR (δ (ppm)): 19.9 ppm. X-ray powder diffraction does not show any bands, which indicated the formation of an amorphous material. XPS analysis: O (43.02%), C (35.08%), Si (11.37%), B (10.53%). The binding energies are as follows: C 1s 285 eV, O 1s 534 eV, Si 2p 105 eV, and B 1s 194 eV.

Preparation of Xerogels X2. The preparation of xerogels was carried out similarly. The procedure for **X2A** is given as an example. In a tube, 327 mg (0.43 mmol) of **P2** was dissolved in 0.43 mL of dried THF containing 13 μL (13 μmol) of TBAF and 34 μL (1.93 mmol) of H_2O. Then the mixture was stirred for 10 s. After 20 min a gel was formed and kept 7 days for aging. The gel obtained was powered and washed three times with ethanol, acetone, and diethyl ether and dried in a vacuum for 3 h to yield 129 mg of an off-white power. Yield: ≈99%, calculated taking into account the total condensation and that carborane has been completely removed (see ideal formula in Scheme 2). FTIR (KBr, cm^{-1}): ν $(C-H)_{alkyl}$ 2966−2912, δ (Si−C) 1267, ν (Si−O−Si) 1037, 694. ^{29}Si CP MAS NMR (δ ppm, 60 MHz): 13.2 (CH_2**Si**−O−**Si**CH_2), − 57.3 (T^2), −64.4 (T^3). ^{13}C CP MAS NMR (δ (ppm)): 59.0 (O−$\mathbf{C}H_2$), 18.3 ($CH_2-\mathbf{C}H_3$), 6.4 (br, Si−$\mathbf{C}H_2$). S_{Bet} = 570 m^2 g^{-1}, average pore diameter = 32 Å. The X-ray powder diffraction does not show any Bragg's peaks.

X2B. In a tube, 203 mg (0.27 mmol) of **P2** was dissolved in 0.27 mL of dried THF containing 0.33 mg (8.1 μmol) of NaOH and 22 μL (1.22 mmol) of H_2O to give 16 mg of a gel after 1824 h. Yield: 22%, calculated taking into account the total condensation and that carborane has been completely removed (see ideal formula in Scheme 2). FTIR (KBr, cm^{-1}): ν $(C-H)_{alkyl}$ 2972−2912, δ (Si−C) 1267, ν (Si−O−Si) 1076, 1027, 694. ^{29}Si CP MAS NMR (δ ppm, 60 MHz): 13.2 (CH_2**Si**−O−**Si**CH_2), −46.1 (T^0), −53.3 (T^1), −57.5 (T^2), −64.7 (T^3). ^{13}C CP MAS NMR (δ (ppm)): 59.0 (O−$\mathbf{C}H_2$), 18.3 ($CH_2-\mathbf{C}H_3$), 6.4 (Si−$\mathbf{C}H_2$). The X-ray powder diffraction does not show any Bragg's peak.

X2C. One hundred ninety milligrams (0.25 mmol) of **P2** in 0.25 mL of dried THF containing 11 μL (0.11 mmol) of HCl (32%) and 20 μL (1.13 mmol) of H_2O gave 79 mg of a gel after 744 h. Yield: 74%. FTIR (KBr, cm^{-1}): ν $(C-H)_{alkyl}$ 2972−2942, δ (Si−C) 1267, ν (Si−O−Si) 1076, 1027, 694. ^{29}Si CP MAS NMR (δ ppm, 60 MHz): 12.0 ($\mathbf{C}_c-$**Si**), −51.5 (T^1), −57.1 (T^2), −64.3 (T^3). ^{13}C CP MAS NMR (δ (ppm)): 59.0 (O−$\mathbf{C}H_2$), 25.0 ($\mathbf{C}_c-CH_3$), 18.6 ($CH_2-\mathbf{C}H_3$), 0.5−12.0 (br, Si−$\mathbf{C}H_2$). S_{Bet} = <10 m^2 g^{-1}. X-ray powder diffraction shows two broad bands with *d* spacings of 16.4 and 6.7 Å.

Preparation of Xerogels X3. The preparation of the xerogels was carried out according to the following general procedure, the **X3A** is given as an example. In a tube, 426 mg (0.52 mmol) of **P3** was dissolved in 0.52 mL of dried THF containing 15.6 μL (15.6 of TBAF and 42 μL (2.34 mmol) of H_2O. Then the mixture was stirred for 10 s. After 25 min a gel was formed and kept 7 days for aging. The gel obtained was powdered and washed three times with ethanol, acetone, and diethyl ether and dried to yield 134 mg as a slightly white powder. Yield: 93%, calculated taking into account the total condensation and that carborane has been completely removed (see ideal formula in Scheme 2). FTIR (KBr, cm^{-1}): ν (O−H) 3365, ν $(C-H)_{alkyl}$ 2974−2889, δ (Si−C) 1265, ν (Si−O−Si) 1053, 694. ^{29}Si CP MAS NMR (δ ppm, 60 MHz): 13.6 (CH_2**Si**−O−**Si**CH_2), −47.0 (T^0) −50.7 (T^1), −57.1 (T^2), −65.0 (T^3). ^{13}C CP MAS NMR (δ (ppm)): 58.9 (O−$\mathbf{C}H_2$), 18.3 ($CH_2-\mathbf{C}H_3$), 6.4 (br, Si−$\mathbf{C}H_2$). S_{Bet} = 170 m^2 g^{-1}, pore size = 28 Å. The X-ray powder diffraction does not show any Bragg's peaks.

X3B. Three hundred twelve milligrams (0.38 mmol) of **P3** in 0.38 mL of THF containing 0.46 mg (11.4 μmol) of NaOH and 31 μL (1.71 mmol) of H_2O gave 73 mg of a gel after 648 h. Yield: 69%, calculated taking into account the total condensation and that carborane has been completely removed (see ideal formula in Scheme 2). FTIR (KBr, cm^{-1}): ν (O−H) 3386, ν $(C-H)_{alkyl}$ 2974−2889, δ $(C-H)_{alkyl}$ 1460, δ (Si−C) 1265, ν (Si−O−Si) 1072. ^{29}Si CP MAS NMR (δ ppm, 60 MHz): 13.6 (CH_2**Si**−O−**Si**CH_2), −49.9 (T^1), −57.0 (T^2), −64.9 (T^3). ^{13}C CP MAS NMR (δ (ppm)) = 58.9 (O−$\mathbf{C}H_2$), 18.3 ($CH_2-\mathbf{C}H_3$), 6.4 (Si−$\mathbf{C}H_2$). The X-ray powder diffraction does not show any Bragg's peaks. Elemental analysis calculated for $C_6H_{12}O_5Si_4$: C, 26,06; H, 4.37. Found: C, 21,83; H, 5.79.

X3C. Three hundred sixty-two milligrams (0.44 mmol) of **P3** in 0.44 mL of THF containing 20 μL (0.20 mmol) of HCl (32%) and 36 μL (1.08 mmol) of H_2O gave 143 mg of a gel after 1296 h. Yield: 67%. FTIR (KBr, cm^{-1}): ν $(C-H)_{alkyl}$ 2958−2928, ν (B−H) 2590, δ $(C-H)_{alkyl}$ 1460, ν (Si−O−Si) 1101. ^{29}Si CP MAS NMR (δ ppm, 60 MHz): 12.2 ($\mathbf{C}_c-$**Si**), −57.0 (T^2), −64.1 (T^3). ^{13}C CP MAS NMR (δ (ppm): 130.5 ($\mathbf{C}_6H_5$), 83.5 ($\mathbf{C}_c$), 58.4 ($SiO\mathbf{C}H_2$), 18.2 ($CH_2\mathbf{C}H_3$), 6.2 ($\mathbf{C}H_2$). S_{Bet} = <10 m^2 g^{-1}. X-ray powder diffraction shows two broad bands with *d* spacings of 16.5 and 6.9 Å.

Acknowledgment. This work has been supported by MCyT, MAT2004-01108, and Generalitat de Catalunya, 2001/SGR/00337. A.G. thanks MCyT for a FPI grant annexed to MAT01-1575.

Supporting Information Available: Various NMR spectra of **P1**−**P3**. This material is available free of charge via the Internet at http://pubs.acs.org.

CM060648W